Geophysical Research Letters

RESEARCH LETTER
10.1029/2018GL078678

Key Points:
- The equatorward shift of the Pacific jet in winter reduces eddy activity and contributes to a midwinter minimum
- Reanalysis data and simulations show that when the January Pacific jet is more poleward, eddy kinetic energy increases
- Zonally symmetric simulations with Pacific temperatures reproduce a midwinter minimum-like behavior in eddy kinetic energy

Supporting Information:
- Figure S1
- Supporting Information S1

Correspondence to:
J. Yuval,
yaniyuval@gmail.com

Citation:
Yuval, J., Afargan, H., & Kaspi, Y. (2018). The relation between the seasonal changes in jet characteristics and the Pacific midwinter minimum in eddy activity. *Geophysical Research Letters*, *45*, 9995–10,002. https://doi.org/10.1029/2018GL078678

Received 28 JAN 2018
Accepted 23 JUN 2018
Accepted article online 3 JUL 2018
Published online 26 SEP 2018

The Relation Between the Seasonal Changes in Jet Characteristics and the Pacific Midwinter Minimum in Eddy Activity

J. Yuval[1], **H. Afargan**[1], **and Y. Kaspi**[1]

[1] Department of Earth and Planetary Sciences, Weizmann Institute of Science, Rehovot, Israel

Abstract This study relates the occurrence of the midwinter minimum in eddy activity over the North Pacific with the seasonality in jet characteristics. During winter, the Pacific jet core is typically around latitude 32°N and has features of a merged subtropical eddy-driven jet. On the other hand, during transition seasons, the jet is at higher latitudes (≈40°N) and resembles more an eddy-driven jet. We find that these differences in jet characteristics play a role in the occurrence of the midwinter minimum. It is found that a midwinter minimum-like behavior in eddy activity, as observed, is obtained in idealized simulations where zonally symmetric temperature profiles are adjusted to mimic the seasonality of longitudinally averaged temperature observed across the North Pacific. Furthermore, we find in both reanalysis data and the idealized simulations that a poleward shift of the January jet leads to an increase in eddy kinetic energy.

Plain Language Summary The Pacific jet transitions from a more northward (approximately latitude 40°N) jet during spring and fall to a stronger, more subtropical, jet (approximately latitude 32°N) during midwinter. It has been well known that the Pacific storm track intensity undergoes a minimum during midwinter. The fact that the Pacific jet is strongest in midwinter while the eddies (storm track) are at a temporal minimum has been a major puzzle. Here we propose that the jet's natural seasonal transition from a more northern eddy-driven jet state to a more subtropical state results in less eddies during midwinter. Our results imply that when the northern Pacific jet shifts poleward and has an eddy-driven jet characteristic, eddy activity strengthens. Conversely, when the jet resembles a subtropical jet, eddy activity weakens. We show that the equatorward shift of the north Pacific jet during midwinter contributes to the presence Pacific midwinter minimum in eddy activity.

1. Introduction

Linear theories of baroclinic instability (Charney, 1947; Eady, 1949) contributed significantly to the understanding of synoptic-scale storms in the midlatitudes. These linear theories provided a scaling that relates climatological eddy amplitude with climatological background flow. This linear relation has been commonly used and shown to be useful in many studies (e.g., Ioannou & Lindzen, 1986; Nakamura & Shimpo, 2004; Li & Battisti, 2008; Thompson & Barnes, 2014). Despite the success of linear theory to explain many phenomena in midlatitudes, the midwinter minimum (MWM) of the Pacific storm track in the Northern Hemisphere remains a remarkable example of the limitations of the linear theory to give a correct prediction to the relation between the mean state and eddies.

Nakamura (1992) was the first to show that the intensity of baroclinic wave activity exhibits a MWM above the North Pacific. This observation is inconsistent with linear instability theories since baroclinicity measures are on average largest in January, while the eddy kinetic energy (EKE) is at a local minimum during midwinter. Nakamura (1992) showed that baroclinic wave amplitude is positively correlated to jet strength when it is below 45 m/s, and it is negatively correlated at higher jets velocities, both on seasonal through interannual time scales (see also Zhang & Held, 1999; Chang, 2001). Nakamura (1992) suggested a few possible explanations that might contribute to the MWM, such as wave trapping, interactions between planetary waves and baroclinic waves, reduction in seeding of baroclinic waves crossing the cold Asian continent in winter, stronger advection of eddies in regions of large baroclinicity, and high specific humidity during spring and autumn which acts to increase the effective baroclinicity. Since the pioneering work of Nakamura (1992), many studies examined different physical mechanisms that could explain the presence of the MWM.

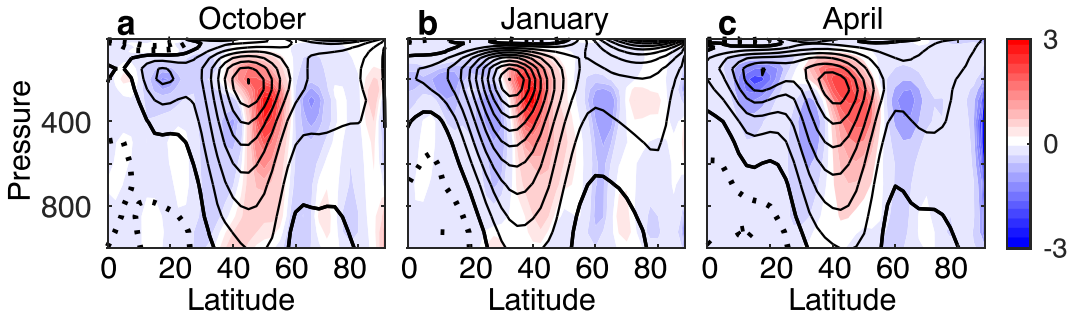

Figure 1. Zonal wind in (a) October, (b) January, and (c) April averaged for the years 1981–2014 (contours, contour intervals 5 m/s), and red and blue colors represent eddy momentum flux convergence and divergence, respectively ($\times 10^5$ m/s^2) for the zonally averaged North Pacific (longitudes 160°E–137.5°W) calculated from the National Centers for Environmental Prediction Reanalysis 2 data. The bold contour is the zero wind line. Dotted lines represent the easterlies.

Nakamura and Sampe (2002) used reanalysis data to show that in winter periods of an intense subtropical jet (STJ), eddies are trapped within its core, away from the strong surface temperature gradients, leading to eddy activity suppression. Harnik and Chang (2004) showed using a channel model, and in a linear model on a sphere, that linear theory can be consistent with the MWM when considering the meridional structure of the jet. They concluded that strong advection alone cannot explain the slower growth rate in winter, but when considering the narrowing of the jet that occurs in winter, the growth rate reduces. Deng and Mak (2005) suggested that the increased local baroclinicity in midwinter could act like a generalized barotropic governor mechanism (James, 1987) and lead to a decrease in the EKE. Penny et al. (2010) used feature-tracking techniques to show that the MWM can be related to the reduction of disturbances entering the Pacific storm track from Asia during winter compared to transition season. Park et al. (2010) and Lee et al. (2013) showed that the presence of the Tibetan Plateau tends to suppress storm track activity in the Pacific midwinter. Yuval and Kaspi (2016) showed in an idealized general circulation model (GCM) with a reconstructed Pacific temperature profile that when the January temperature profile is simulated, the EKE is less than in simulations with the zonally symmetric temperature distributions for April and November.

In this study, we relate seasonally different characteristics of the midlatitude jet over the North Pacific with the occurrence of the MWM in eddy activity. Over the North Pacific, the jet stream exhibits a pronounced seasonal cycle. In transition seasons, a double jet structure is present (Figures 1a and 1c). At lower latitudes (≈20°N), a STJ is found where eddy momentum flux is divergent and thus indicative of eddy deceleration of the mean flow (Figures 1a and 1c). At higher latitudes (≈40°N), an eddy-driven jet (EDJ) is found where eddy momentum flux is convergent and thus indicative of eddy acceleration of the mean flow. On the other hand, during winter, there is a single jet located at latitude ≈32°N, which shows mixed characteristics of STJ and EDJ (Figure 1b; see also Eichelberger & Hartmann, 2007, and Figure 1 in Li & Wettstein, 2012, where it is shown that the zonal wind in winter exhibits more characteristics of a thermally driven jet and less of those of an EDJ than in transition season, implying that the jet has a more subtropical nature in winter than in transition seasons). Lachmy and Harnik (2014) showed that in a STJ regime eddies tend to be weaker than in a case of an EDJ regime. In this study, we show that the transition between the jet types might play an important role in the presence of the MWM.

Using reanalysis data, we show that during winter, there is correlation between the jet latitudinal position and EKE. In time periods when the jet is more poleward, EKE is larger. We demonstrate that a MWM-like EKE pattern can be obtained in an idealized GCM that mimics longitudinally averaged temperature distributions observed across the North Pacific in individual calendar months. This implies that the seasonal differences in latitudinal temperature profiles over the North Pacific can be a viable mechanism for the occurrence of the MWM. Moreover, we demonstrate in a set of zonally symmetric simulations that a poleword shift of a January-like jet (similar to what occurs in transition seasons) leads to EKE increase. All these findings imply that the differences in jet characteristics between winter and transition seasons, and specifically the equatorward jet shift in winter, may play an important role in the presence of the MWM. Previous studies (Lee et al., 2013;Nakamura, 1992; Park et al., 2010; Penny et al., 2010, 2011, 2013) suggested that zonal asymmetries and changes in the role of latent heat release, which during transition seasons acts to generate eddy available potential energy while during winter it dissipates eddy available potential energy (Chang, 2001), could be the underlying

reason that leads to the MWM. Our results imply that the zonally symmetric dry dynamics have the necessary complexity to reproduce a Pacific MWM and that neither zonal asymmetries or moisture is a necessary condition for the presence of the MWM. Nevertheless, the temperature profile above the Pacific is a consequence of complicated dynamics, which is affected by latent heat and zonal asymmetries. Therefore, though not explicitly represented in the model, the effects of zonal asymmetries and latent heat can influence the simulations implicitly through the observed climatological temperature field, which is specified in the model. Furthermore, Chang and Zurita-Gotor (2007) used an idealized model with a temperature distribution that resembled the monthly mean 3-D temperature distribution of the entire Northern Hemisphere. Although they were able to reproduce the seasonal cycle of mean flow structure over the Pacific, they were unable to obtain a MWM in the storm track intensity. This suggests that changing the jet structure alone may be insufficient to explain the MWM in a more realistic three-dimensional setting, and the reproduction of the MWM in the idealized simulations does not imply that the other mechanisms mentioned above are less important than the proposed mechanism in this paper.

The paper is organized as follows. The GCM and the relaxation scheme are discussed in section 2, as well as how the relaxation temperature profiles are obtained and details of the observational data that is used. In section 3.1, we present the results of the simulations, which show that a Pacific MWM can be obtained using this GCM configuration. In section 3.2, it is shown in reanalysis data that in periods when the jet is more poleward, EKE is larger. In section 3.3, we demonstrate in simulations that when the winter jet is shifted poleward (as occurs in transition seasons), EKE tends to increase. In section 4, the results are summarized.

2. Model Description

2.1. Idealized GCM

A dry version of an idealized GCM based on the spectral dynamical core of the Geophysical Fluid Dynamics Laboratory Flexible Modeling System is used. The model is driven by a Newtonian cooling scheme that is described in section 2.3. The simulations do not include orography or ocean. Dissipation in the boundary layer is represented by linear damping of near-surface winds (below $\sigma = 0.7$) with a relaxation time of 1 day at the surface (see Held & Suarez, 1994, for details). The model used for all simulations has 60 vertical sigma levels at T42 horizontal resolution (2.8° × 2.8°). What distinguishes these simulations from Held and Suarez (1994) is the relaxation temperatures and the relaxation time used in the simulations; see sections 2.2 and 2.3.

The simulations are integrated over 2,000 days, where the first 1,000 days are treated as spin-up, and the results are averaged over the last 1,000 days. Simulations in this study are not hemispherically symmetric, and only the northern hemispheric data are analyzed.

2.2. Temperature Profiles in the Simulations

The relaxation temperature profile for a particular calendar month is taken from the monthly climatology of the National Centers for Environmental Prediction Reanalysis 2 data (Kanamitsu et al., 2002, years 1981–2010). Focusing on the North Pacific basin, the temperature is zonally averaged over longitudes of the North Pacific basin (160°E–137.5°W), which leads to a zonally symmetric relaxation temperature. Since the vertical resolution of the GCM used in this study has different vertical resolution than the reanalysis data, the temperature fields are interpolated onto the model levels.

2.3. Forcing on the Mean State

To obtain a North Pacific-like temperature profile in different months in the idealized GCM, a diabatic formulation developed by Zurita-Gotor (2007) is used. The main difference between the Newtonian cooling scheme that is used in this study and the formulation that is commonly used in idealized studies is the usage of different relaxation time scales for the eddies and the zonal mean. The temperature equation in this formulation can be written as

$$\partial_t T = \ldots - \alpha_T (T - \overline{T}) - \alpha_T \gamma (\overline{T} - \overline{T_R}), \tag{1}$$

where α_T^{-1} is the relaxation time of eddies, which is chosen to be 20 days at all vertical levels (uniform relaxation time), and T_R is the relaxation temperature, which is taken to be the target temperature taken from the reanalysis data at every month. $\alpha_T^{-1}\gamma^{-1}$ is the relaxation time for the mean state, where we take $\gamma = 100$, the zonal average of field A is represented by $\overline{A}$, and all advection and diabatic terms except the relaxation terms

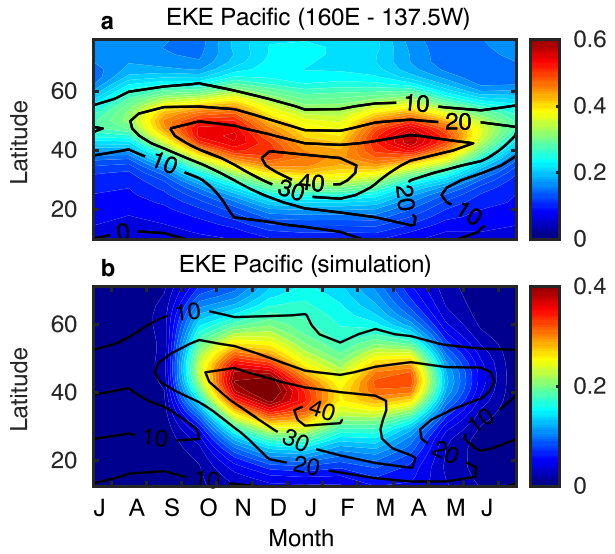

Figure 2. The seasonal cycle of latitudinal profiles of vertically integrated EKE (MJ/m^2, color) and 250 hPa zonal wind (m/s, contour). The abscissa denotes individual calendar months. The mean EKE is calculated as $\frac{1}{2g}\int[v^{*2}+u^{*2}]dp$ ([A] is the zonal average over the Pacific region). The data are taken from the National Centers for Environmental Prediction Reanalysis 2 data averaged between 1982 and 2014 (a) and from zonally symmetric simulations that mimic the North Pacific temperature distribution (b). Note that the color scale is different between the two panels. EKE = eddy kinetic energy.

are omitted in equation (1). The fast relaxation for the mean state is chosen such that it allows reproducing a very similar mean profile to the reanalysis data (with zonal mean deviation of less than 1 K, see supporting information). A discussion regarding the possible drawbacks of strong zonal temperature relaxation can be found in Yuval and Kaspi (2017).

2.4. EKE Calculation and Reanalysis Data

To compare the EKE results of the simulations to observations, the EKE is calculated using a Butterworth bandpass filter with cutoff periods of 3 and 10 days. The wind data are taken from the National Centers for Environmental Prediction Reanalysis 2 data set, using 6-hourly fields of horizontal winds between 1981 and 2014, and are zonally averaged in the Pacific sector (160°E–137.5°W). This allows comparing the zonally symmetric simulations and zonally asymmetric data.

3. Results

3.1. A Pacific MWM in Zonally Symmetric Simulations With Perpetual Seasons

The latitude-time diagram of the vertically integrated EKE calculated from the reanalysis data is plotted in Figure 2a and a similar figure for the zonally symmetric simulations in Figure 2b. In both the reanalysis data and the simulations, there is a clear MWM in the EKE, although the local maximum in the EKE appears in November and December in the simulations, while in the reanalysis data the maximum appears also in October. Another similarity between the simulations and the reanalysis data is that at higher latitudes, poleward of 60°N, the EKE is larger in winter than in transition seasons.

There are several differences between the reanalysis data and the simulations. First, during winter and transition seasons, the EKE is smaller by approximately 30% in the simulations compared to the reanalysis data. Similar discrepancy in EKE magnitude between reanalysis data and an idealized GCM with realistic temperature distribution was also found by Chang (2006) and Yuval and Kaspi (2016). Since the idealized GCM is missing a lot of realistic physical aspects, it is not expected to reproduce the reanalysis-based statistics quantitatively. Rather, the focus of this study is on the qualitative aspects of the simulations. Furthermore, the EKE magnitude in the simulations is affected by various model parameters (e.g., relaxation time scale), so its value is not determined solely by the prescribed temperature distribution. Second, from May to September, the EKE in the simulations is nearly 0, which is substantially different from the reanalysis data. It is possible that latent heat effects and zonal asymmetries play an important role in exciting and enhancing instabilities in these months, and the absence of these effects in the model causes negligible EKE. Third, EKE in the sim-

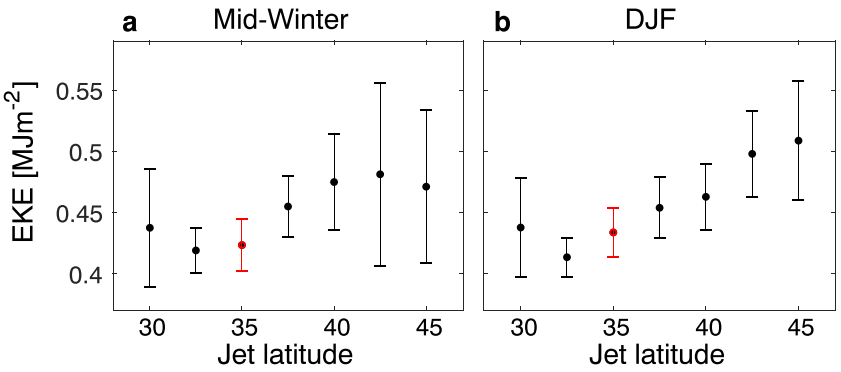

Figure 3. The relation between the vertically and horizontally integrated EKE (MJ/m^2) as a function of jet latitude during midwinter (a, 15 December to 14 February) and during DJF (b, 1 December to 28 February). The jet latitude is determined by the maximum zonal wind for 31-day running mean sampled at 10-day intervals for the years 1982–2014. Confidence intervals of 95% are marked by the lines, and the climatological-mean position of the jet is indicated by the red dot. EKE = eddy kinetic energy; DJF = December-January-February.

ulations during fall is significantly larger than in spring. This difference is not present in the reanalysis data. This implies that the idealized model with the zonally symmetric Pacific temperature distribution does not have the necessary complexity in order to reproduce accurately the EKE differences between the transition seasons.

3.2. The Relation Between Jet Latitude and the Storm Track—Reanalysis Data

The relation between the EKE and the jet latitude in the Pacific sector is plotted in Figure 3. For each year between 1982 and 2014, a 31-day running mean of the zonal wind and the EKE was calculated, sampled at 10-day intervals. EKE was averaged over all time periods during midwinter (panel a) and during December-January-February (panel b), in which the jet was located at a certain latitude (excluding latitudes with less than three time periods of maximal jet). The jet latitude was determined as the maximum of the vertically and horizontally (160°E–137.5°W) averaged zonal wind during each time period. The EKE was calculated as a vertical and horizontal average over a ±10° latitude interval centered around the latitude of EKE maximum. Figure 3 shows that during winter, the EKE is smaller in periods when the jet is located at low latitudes and increases when the jet is located more poleward (with the exception of the equatorward most point in both panels, though these points have a large confidence intervals). This implies that the latitudinal position of the Pacific jet during winter is correlated with the decreased EKE. These results are consistent with Nakamura et al. (2002) and Nakamura and Sampe (2002), who found that in winters where the jet is located more equatorward than its climatological mean the MWM is more pronounced, and with Afargan and Kaspi (2017), who showed that in years when the Atlantic jet is stronger and more equatorward than its climatological-mean state a MWM of EKE occurs in the Atlantic as well.

3.3. Seasonal Baroclinicity Differences in Simulations

The meridional temperature gradient (Figures 4a–4c) and the Eady growth rate (Figures 4d–4f) are plotted for simulations with the Pacific temperature profile of November, January, and April. In both transition seasons, there is a decrease in the meridional temperature gradient and Eady growth rate around 30°N, which corresponds to the climatological jet position in January, alongside a local increase in temperature gradient and Eady growth rate at the poleward flank of the jet (Figures 4a, 4c, 4d, and 4f), especially in the upper troposphere around 45°N. In January, the meridional temperature gradient is concentrated more equatorward than in transition seasons as a result of a seasonally strengthened Hadley cell, which creates a strong merged subtropical EDJ.

To consider if a jet is more subtropical or more eddy-driven, we focus on the distance between the jet maximum and the Ferrel's cell center (the larger the distance, the more similar is the jet to a STJ). Figures 4g–4i show that the jet's maximum is farthest from the center of the Ferrel cell in January, implying that the jet in the January simulation is a more subtropical-like jet than during transition seasons.

To investigate the role of the poleward shift of the jet in transition seasons in comparison to January, a set of simulations was conducted. Namely, the January temperature profile was modified at midlatitudes

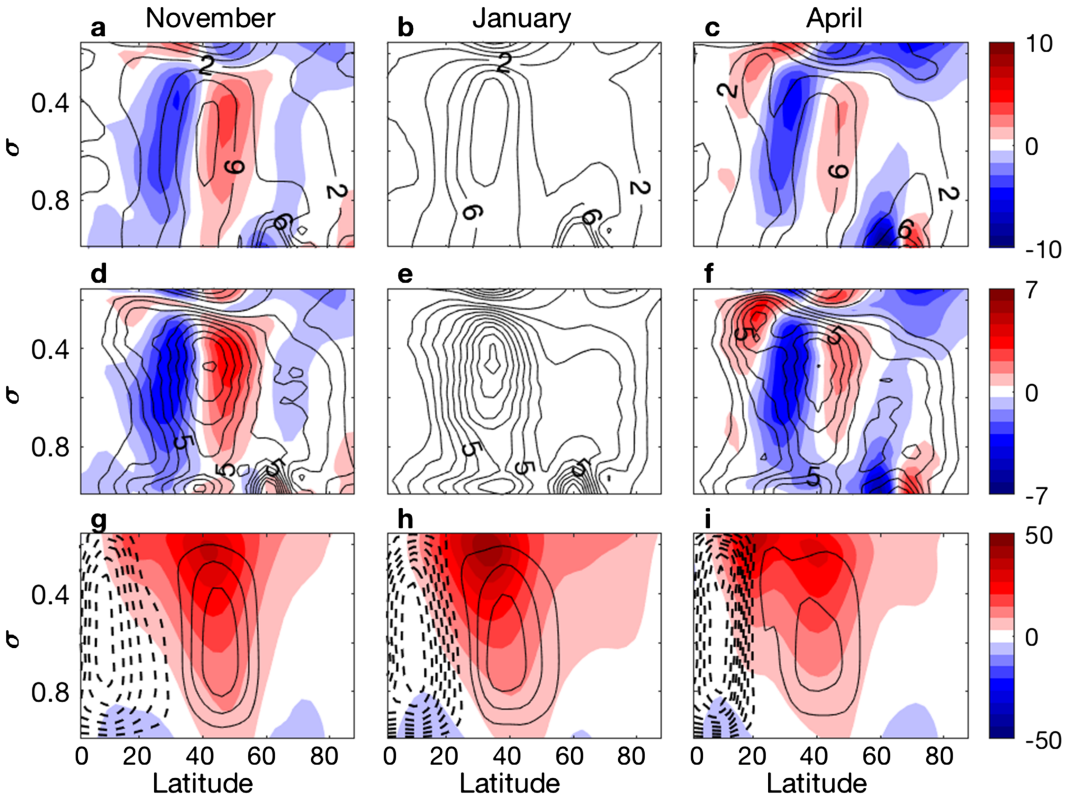

Figure 4. The meridional temperature gradient $\times 10^6$ (K/m, a–c) and Eady growth rate $\times 10^6$ (s^{-1}, d–f) for zonally symmetric simulations with November, January, and April conditions. Colors indicate the differences from January, and contours are the values of the different fields. The contour intervals are 2 K/m (temperature gradient) and 1 s^{-1} (Eady growth rate). In panels (g–i) ,the streamfunction (contours intervals 12 kg/s $\times 10^9$) and wind (m/s, colors) are plotted for each simulation separately.

so as to mimic the situation in the transition seasons. Specifically, the induced temperature changes include a poleward jet shift relative to January. The temperature changes can be expressed in the following way:

$$T_{\text{Jan-tran}} = T_{\text{Jan}} + (T_{\text{tran}} - T_{\text{Jan}})e^{-\frac{(\phi-\phi_c)^2}{2\phi_d^2} - \frac{(\sigma-\sigma_c)^2}{2\sigma_d^2}}, \quad (2)$$

where $\phi_c = 36°$ is the center latitude that the change in temperature occurs, $\phi_d = 10°$ is the typical latitudinal width of the change, $\sigma_c = 0.63$ is the vertical level at which the change maximizes, $\sigma_d = 0.3$ is a measure of the depth of the change, T_{Jan} is the longitudinally averaged Pacific January temperature profile, and T_{tran} is the temperature profile in the transition seasons specified separately for April, October, and November. The choice of parameters was made so as to simulate a poleward jet shift (as occurs during transition seasons), such that there will be similarity between the observed gradient differences in midlatitudes and the simulated ones. The temperature (Figures 5a–5c), wind (Figures 5d–5f), and EKE (Figures 5g–5i) differences between January and the modified January profile (equation (2)) are plotted in Figure 5. The induced temperature changes lead to a weakening of the jet at its equatorward flank and strengthening at its poleward flank, where the temperature change is larger in fall than in spring (Figures 5a–5c). Therefore, January spring-like simulations have a weak poleward shift of the jet (Figure 5f) and, consequently, only a small change in the mean EKE (Figure 5i). Conversely, the January fall-like simulations have a large shift in the temperature gradient and a large increase in EKE (Figures 5g and 5h). This response of EKE implies that as the January jet shifts poleward, EKE increase. These results are consistent with Yuval and Kaspi (2018), who showed in an idealized GCM that a poleward shift of the jet tends to increase EKE. Furthermore, when the January jet is shifted poleward, regions of large upper level baroclinicity and of large lower level baroclinicity (which are found at higher latitudes) tend to be spatially closer, which tends to intensify eddy activity (Nakamura & Sampe, 2002). To verify that the results are not sensitive to the choice of ϕ_c, additional simulations with the value $\phi_c = 42°$ were performed, and the results remain qualitatively similar.

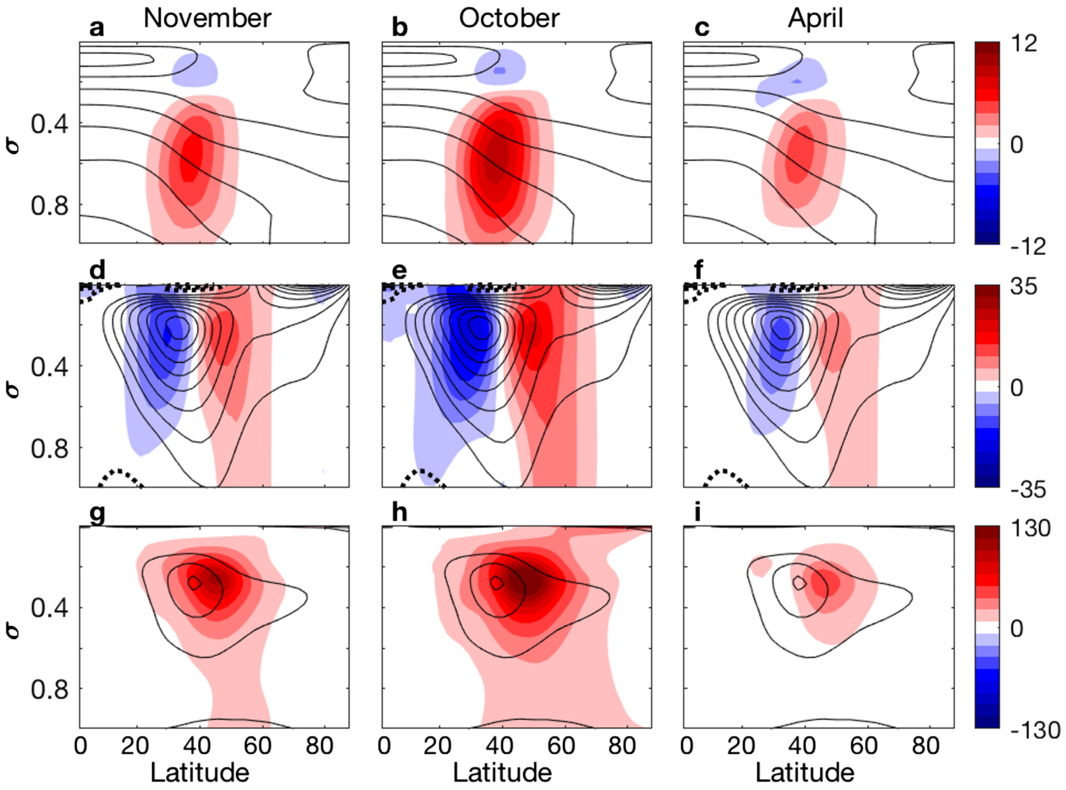

Figure 5. Temperature (K, a–c), zonal wind (m/s, d–f), and EKE (m^2/s^2, g–i) for simulations where the January temperature profile was modified as in equation (2). Contours show the January reference, and the colors represent deviations from this reference. The contour intervals are 15 K (temperature), 5 m/s (zonal wind), and 25 m^2/s^2 (EKE). EKE = eddy kinetic energy.

4. Discussion and Summary

In this study, we argue that the different jet characteristics between winter and the transition seasons could play a role in the MWM presence. During winter, the jet is located at lower latitudes and has features of a merged subtropical EDJ, while during the transition seasons, the jets are more separated, and the poleward jet resembles an EDJ (Figure 1). To investigate this hypothesis, we use both reanalysis data and an idealized GCM. It is found in the reanalysis data that in time periods during winter in which the jet is located more poleward, the EKE is larger (Figure 3).

The simulations show that when the mean Pacific temperature field is simulated in different months, the EKE exhibits a MWM-like behavior (Figure 2b). This implies that the seasonality in meridional temperature profile over the North Pacific (which is profoundly related to the jet structure via thermal wind balance) plays an important role in the MWM occurrence.

To investigate the effect of poleward shift of the January jet on EKE, the idealized GCM was used to simulate temperature profiles that are similar to January but with a poleward shifted jet (such that the jet is more similar to a transition season jet). It is found that when the January jet is shifted poleward, EKE tends to increase (Figure 5). These results imply that the jet position and its characteristics play an important role in determining the EKE amplitude and on the presence of the MWM. Futhermore, these simulated results are consistent also with Nakamura et al. (2002) and Nakamura and Sampe (2002), who found that not only the seasonal but also the interannual modulations in the strength of MWM are correlated with a stronger and more equatorward jet.

Acronyms

EDJ Eddy-driven jet
EKE Eddy kinetic energy

GCM General circulation model
MWM Midwinter minimum
STJ Subtropical jet

Acknowledgments
We thank the two reviewers for their very constructive comments that helped to improve the quality of this work. NCEP Reanalysis data are provided by the NOAA/OAR/ESRL PSD, Boulder, Colorado, USA (http://www.esrl.noaa.gov/psd). This research has been supported by the Israeli Science Foundation (grant 1819/16).

References

Afargan, H., & Kaspi, Y. (2017). A midwinter minimum in North Atlantic storm track intensity in years of a strong jet. *Geophysical Research Letters*, *44*, 12,511–12,518. https://doi.org/10.1002/2017GL075136

Chang, E. K. M. (2001). GCM and observational diagnoses of the seasonal and interannual variations of the Pacific storm track during the cool season. *Journal of the Atmospheric Sciences*, *58*, 1784–1800.

Chang, E. K. M. (2006). An idealized nonlinear model of the Northern Hemisphere winter storm tracks. *Journal of the Atmospheric Sciences*, *63*, 1818–1839.

Chang, E. K. M., & Zurita-Gotor, P. (2007). Simulating the seasonal cycle of the Northern Hemisphere storm tracks using idealized nonlinear storm-track models. *Journal of the Atmospheric Sciences*, *64*(7), 2309–2331.

Charney, J. G. (1947). The dynamics of long waves in a baroclinic westerly current. *Journal of Meteorology*, *4*, 136–162.

Deng, Y., & Mak, M. (2005). An idealized model study relevant to the dynamics of the dynamics of the midwinter minimum of the Pacific storm track. *Journal of the Atmospheric Sciences*, *62*, 1209–1225.

Eady, E. T. (1949). Long waves and cyclonic waves. *Tellus*, *1*, 33–52.

Eichelberger, S. J., & Hartmann, D. L. (2007). Zonal jet structure and the leading mode of variability. *Journal of Climate*, *20*, 5149–5163.

Harnik, N., & Chang, E. K. M. (2004). The effects of variations in jet width on the growth of baroclinic waves: Implications for midwinter Pacific storm track variability. *Journal of the Atmospheric Sciences*, *61*, 23–40.

Held, I. M., & Suarez, M. J. (1994). A proposal for the intercomparison of the dynamical cores of atmospheric general circulation models. *Bulletin of the American Meteorological Society*, *75*, 1825–1830.

Ioannou, P., & Lindzen, R. S. (1986). Baroclinic instability in the presence of barotropic jets. *Journal of the Atmospheric Sciences*, *43*(2), 2999–3014.

James, I. N. (1987). Suppression of baroclinic instability in horizontally sheared flows. *Journal of the Atmospheric Sciences*, *44*, 3710–3720.

Kanamitsu, M., Ebisuzaki, W., Woollen, J., Yang, S.-K., Hnilo, J., Fiorino, M., & Potter, G. (2002). NCEP–DOE AMIP-II Reanalysis (R-2). *Bulletin of the American Meteorological Society*, *83*(11), 1631–1643.

Lachmy, O., & Harnik, N. (2014). The transition to a subtropical jet regime and its maintenance. *Journal of the Atmospheric Sciences*, *71*, 1389–1409.

Lee, S. S., Lee, J. Y., Ha, K. J., Wang, B., Kitoh, A., & Kajikawa, Y. (2013). Role of the Tibetan Plateau on the annual variation of the mean atmospheric circulation and storm-track activity. *Journal of Climate*, *26*, 5270–5286.

Li, C., & Battisti, D. S. (2008). Reduced Atlantic storminess during Last Glacial Maximum: Evidence from a coupled climate model. *Journal of Climate*, *21*, 3561–3579.

Li, C., & Wettstein, J. J. (2012). Thermally driven and eddy-driven jet variability in reanalysis. *Journal of Climate*, *25*(5), 1587–1596.

Nakamura, H. (1992). Midwinter suppression of baroclinic wave activity in the Pacific. *Journal of the Atmospheric Sciences*, *49*, 1629–1642.

Nakamura, H., Izumi, T., & Sampe, T. (2002). Interannual and decadal modulations recently observed in the Pacific storm track activity and East Asian winter monsoon. *Journal of Climate*, *15*(14), 1855–1874.

Nakamura, H., & Sampe, T. (2002). Trapping of synoptic-scale disturbances into the North-Pacific subtropical jet core in midwinter. *Geophysical Research Letters*, *29*(16), 1761. https://doi.org/10.1029/2002GL015535

Nakamura, H., & Shimpo, A. (2004). Seasonal variations in the Southern Hemisphere storm tracks and jet streams as revealed in a reanalysis dataset. *Journal of Climate*, *17*, 1828–1844.

Park, H., Chiang, J. C. H., & Son, S. (2010). The role of the central Asian mountains on the midwinter suppression of North Pacific storminess. *Journal of the Atmospheric Sciences*, *67*, 3706–3720.

Penny, S., Battisti, D. S., & Roe, G. H. (2013). Examining mechanisms of variability within the Pacific storm track: Upstream seeding and jet-core strength. *Journal of Climate*, *26*, 5242–5259.

Penny, S., Roe, G. H., & Battisti, D. S. (2010). The source of the midwinter suppression in storminess over the North Pacific. *Journal of Climate*, *23*, 634–648.

Penny, S., Roe, G. H., & Battisti, D. S. (2011). Reply to comments on "The source of the midwinter suppression in storminess over the North Pacific". *Journal of Climate*, *24*, 5192–5194.

Thompson, D. E. J., & Barnes, E. A. (2014). Periodic variability in the large-scale Southern Hemisphere atmospheric circulation. *Science*, *343*, 641–645.

Yuval, J., & Kaspi, Y. (2016). Eddy activity sensitivity to changes in the vertical structure of baroclinicity. *Journal of the Atmospheric Sciences*, *73*, 1709–1726.

Yuval, J., & Kaspi, Y. (2017). The effect of vertical baroclinicity concentration on atmospheric macroturbulence scaling relations. *Journal of the Atmospheric Sciences*, *74*(5), 1651–1667.

Yuval, J., & Kaspi, Y. (2018). Eddy response to changes in jet characteristics. *Journal of the Atmospheric Sciences*, *75*, 1371–1383.

Zhang, Y., & Held, I. M. (1999). A linear stochastic model of a GCM's midlatitude storm tracks. *Journal of the Atmospheric Sciences*, *56*, 3416–3435.

Zurita-Gotor, P. (2007). The relation between baroclinic adjustment and turbulent diffusion in the two layer model. *Journal of the Atmospheric Sciences*, *64*, 1284–1300.